ChemComm

COMMUNICATION

View Article Online
View Journal | View Issue

Cite this: *Chem. Commun.*, 2014, **50**, 13746

Received 8th August 2014,
Accepted 9th September 2014

DOI: 10.1039/c4cc06075j

www.rsc.org/chemcomm

Supported core–shell nanobiosensors for quantitative fluorescence imaging of extracellular pH†

Jérémie Asselin,[ab] Carl Roy,[ab] Denis Boudreau,*[ab] Younès Messaddeq,[b] Rihab Bouchareb[c] and Patrick Mathieu[c]

Covalent "click" cycloaddition was used to functionalize silica substrates with pH-sensitive nanoparticles, thus producing uniform and highly luminescent analytical devices usable in both commercial fluorimeters and fluorescence microscopes. Quantitative and spatially-resolved extracellular pH measurements were successfully achieved on live cardiac fibroblasts with these novel ion-sensitive surfaces.

The quantitative measurement of physiological ions near biological membranes is crucial for the investigation of cellular metabolic pathways. For example, the determination of ion concentrations across cell membranes is primordial to study the dysregulation of extracellular pH by cancer cells[1] or the role of calcium, sodium and potassium cations in neurons[2] and other excitable cells.[3] Among the techniques available, the use of ion-selective fluorescent markers offers the benefits of being nonintrusive and easily amenable to *in vitro* spatially-resolved measurements. The inherent hydrophobicity of many organic fluorophores and fluorescent nanoparticles allows them to penetrate the phospholipid bilayer and emit cytosolic-characteristic fluorescence, and thus to quantify intracellular concentrations.[4] Because of the diffusion of fluorescent markers through the membrane, however, no similar method is available to quantify the concentration of ions in the extracellular space. A chemical grafting method able to confine ionic sensors to the extracellular medium could provide a solution to these problems through the use of a functionalized substrate directly implantable in the culture medium for *in vitro* studies.

In this work, we used a "click" chemistry synthetic route to attach core–shell luminescent nanoparticles to silica surfaces with complementary silane-based functionalities (Fig. 1). The concentric architecture comprises a silver core with an average diameter of 60 ±10 nm on which a silica shell with a thickness of 9 ±1 nm doped with ion-selective fluorescent molecules is grown (see the ESI† for a detailed description of the synthesis procedures). Ag@SiO_2-FiTC are very robust with regard to fluorophore leaking to the surrounding media, with insignificant losses after being immersed for 16 h in a phosphate buffer solution (see Fig. S1, ESI†). Several authors have shown that the presence of the silver core increases the local electric field intensity and allows efficient coupling between the oscillating electrons in the metal and the surrounding fluorophores. This results in an increase in the radiative rate and brightness, and the shortening of the excited state lifetime by the metal core improves the robustness with regard to quenching and photobleaching, because the faster radiative relaxation competes more effectively with collisional quenching and dissociation processes.[5]

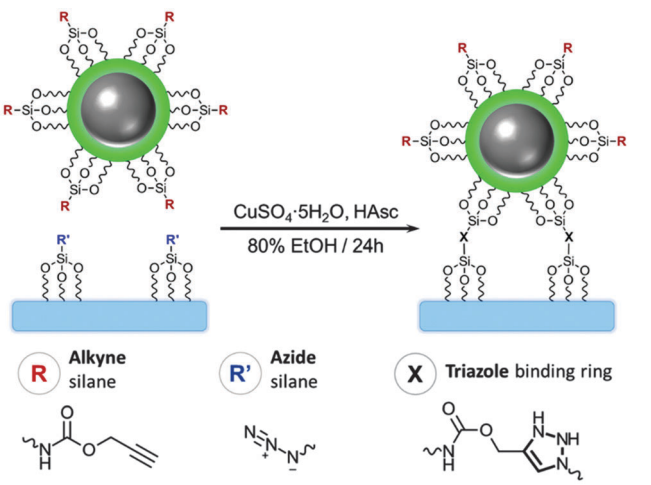

Fig. 1 "Click" coupling scheme used to graft fluorescent silver core–silica shell nanoparticles (Ag@SiO_2-FiTC NPs) onto a SiO_2 substrate. The complementary silane moieties are permutable between both components.

[a] *Département de chimie, Faculté de Sciences et Génie, Université Laval, Québec (QC), Canada G1V 0A6. E-mail: denis.boudreau@chm.ulaval.ca; Fax: +1 418-656-7916; Tel: +1 418-656-3287*

[b] *Centre d'optique photonique et laser (COPL), Université Laval, Québec (QC), Canada G1V 0A6*

[c] *Laboratoire d'études moléculaires des valvulopathies, Institut universitaire de cardiologie et de pneumologie de Québec, Université Laval, Québec (QC), Canada G1V 4G5*

† Electronic supplementary information (ESI) available: Synthesis procedures, UV-Vis and fluorescence spectra of core–shell nanoparticles and pH-sensitive surfaces, fluorescence ratiometry calibration curves and epifluorescence photographs. See DOI: 10.1039/c4cc06075j

Other studies in the literature have employed the "click" grafting of proteins onto the surface of metallic nanoparticles as delivery devices.[6] The method has also been used on lamellar silica substrates to attach antibodies and polysaccharides for surface sensing.[7] The possibility of functionalizing both surfaces separately before combining them using the selective "click" reaction is important; by comparison, other coupling methods (*e.g.*, EDC-NHS) can suffer from secondary reactions that decrease the effective yield. Since the stability of the triazole ring formed by [3+2] cycloadditions is well known on surfaces, various steps were chosen to maximize the homogeneity and luminescence intensity of the final analytical substrate. Ascorbic acid and copper sulfate were used as co-catalysers to generate Cu^{I} *in situ*; this oxidized copper is used to activate the terminal alkyne for the Huisgen cycloaddition.[8] Even if the complementary silane moieties are permutable at will between both the $Ag@SiO_2$ NPs and the silica coverslips, the functionalization of alkyne silanes on core–shell nanoparticles leads to better grafting density whereas modification of the silica shell with the azide silane displays a less stable fixation (Fig. S2-A, ESI†). Although this high accessibility of the alkynes to catalytic Cu^{I} in suspension seems to improve the reaction kinetics and ultimately leads to a more homogeneous grafting, its efficiency was observed to increase rapidly with contact time (Fig. S2-B, ESI†). Binding of non-aggregated nanoparticles was confirmed by SEM and, as such, the fluorescence intensity of the resulting monolayer and its plasmonic extinction were highly uniform and repeatable from substrate to substrate (Fig. 2). In addition to $Ag@SiO_2$ nanoparticles, $Au@SiO_2$ and $In@SiO_2$ NPs, as well as commercial Ludox™ silica particles were also successfully grafted onto lamellar substrates using this strategy (see Fig. S3, ESI†).

Fluorescence measurements were performed with custom-made fluidic cells to study the effect of different biological buffers on the $Ag@SiO_2$-FiTC grafted substrates. Fluorescein derivatives, *e.g.* fluorescein isothiocyanate (FiTC), are well known for having a pH-dependent quantum yield, leading to a linear increase of emission intensity in the physiological pH range ~5–8.[9] Other fluorophores, such as SNARF compounds, would also be suitable for the transduction of pH in our nanosensors,[10] and fluorescein was chosen because of its well-documented chemistry, wide availability and low cost. The versatility of the core–shell architecture, namely the possibility to bind any molecule with reactive moieties to form a fluorescent silane precursor, also allows mixing of distinct emitters on the same device without undesirable RET (resonant energy transfer) crosstalk and better control of the fluorophore-plasmonic core distance, whereas metal islands formed on surfaces are limited in these aspects.[11] To verify this possibility, mixtures of nanobiosensors doped with either FiTC or pH-insensitive eosin isothiocyanate (EiTC) were grafted on the same microscopy coverslips (Fig. 3A). Ratiometric normalization of the FiTC signal by proton non-sensitive EiTC minimizes the influence of instrumental errors (*e.g.*, variations in grafting density or excitation light source intensity) and the response of the nanobiosensors to slight variations in pH tends to demonstrate the capability of small ions to diffuse through the silica shell and modify the local environment of the sensing moieties (Fig. 3B). Therefore, with subtle changes in the synthesis of the fluorescent NPs, it would be possible to use other ion-specific fluorophores and apply ratiometry

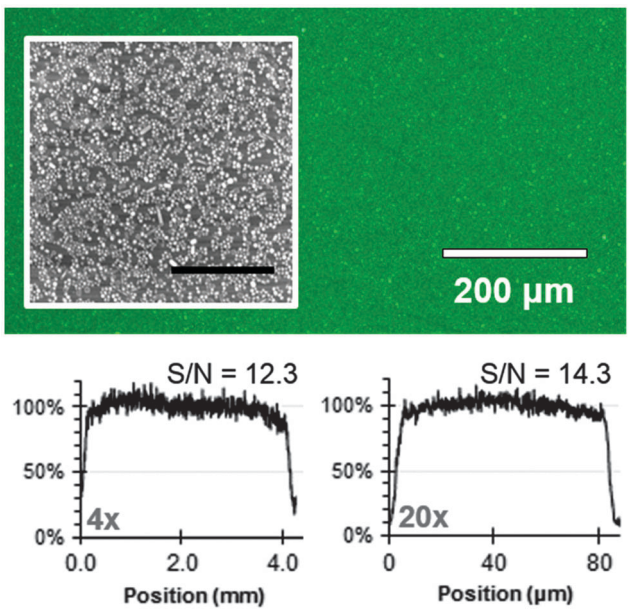

Fig. 2 Up: fluorescence image (λ_{exc} = 489 ± 6 nm, λ_{em} = 536 ± 20 nm) of a ~1 mm^{-2} area on a substrate grafted with $Ag@SiO_2$-FiTC (inset: the SEM image of a representative region of the substrate (scale bar = 1 µm)). Down: fluorescence signal homogeneity across the substrate measured using 4× and 20× microscope objectives (S/N: signal-to-noise ratio).

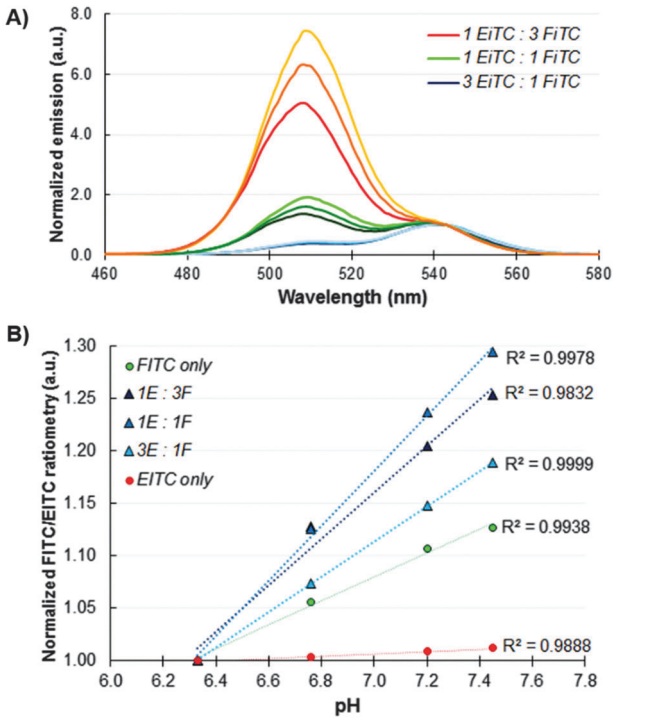

Fig. 3 (A) Fluorescence emission of $Ag@SiO_2$-FiTC and $Ag@SiO_2$-EiTC grafted onto the same coverslip in controlled proportions. Spectra from each color-coded group were measured at pH 6.2, 6.8 and 7.4 (*e.g.*, from bottom to top). Spectra are normalized at EiTC maximum (543 nm); (B) linearity of the FiTC/EiTC ratiometric signal with pH.

for multiplex detection in complex samples with increased sensitivity. Immobilizing two distinct nanoparticle types, *i.e.* Ag@SiO_2-FiTC and Ag@SiO_2-EiTC, on the same substrate rather than a single type of NP doped with both fluorophores would minimize the possibility of energy transfer, since two NPs closer than the Förster distance for the FiTC/EiTC donor–acceptor pair would only allow a limited number of molecules to interact.

The intrinsic ratiometric properties of FiTC have already been used as a viable correction method to minimize experimental errors.[10] The excitation spectrum of FiTC measured at pH values between 6.2 and 7.5 shows an isosbestic point and an inversion of sensitivity to pH at 470 nm (Fig. 4A), with maximum positive and negative sensitivity values recorded at 490 nm and 440–450 nm, respectively (Fig. 4B). The results presented in Fig. 4C show that ratiometric normalization (λ_{exc} = 490/440 nm, λ_{em} = 512 nm) results in a significant increase in sensitivity and linearity of the measurements as compared with measuring at a single excitation wavelength, and could also be used to correct for variations in device response from batch to batch. The procedure can also be easily ported to a fluorescence microscope equipped with appropriate excitation and emission filters (Fig. S4, ESI†). With modern commercial epifluorescence microscopes capable of acquiring two successive images at different excitation wavelengths in as little as 0.2 s, ratiometric normalization can easily be implemented to minimize impact factors such as variations in excitation source intensity.

To demonstrate the use of Ag@SiO_2-FiTC sensing surfaces for the measurement of extracellular pH, human cardiac fibroblasts were grown on a pH-sensitive substrate. This type of cell was chosen because of its good adhesive properties on surfaces in culture media, thus a close proximity between the cellular membrane and the pH-sensitive surface is achieved. The adhesion of the cells everywhere on the functionalized substrates (Fig. S5, ESI†) suggests that protection of plasmonic silver cores with the dye-doped silica shell reduces the leaching of Ag^+ ions (a known cytotoxic species[12]) to tolerable levels. The fibroblasts were transfected with a plasmid incorporating a gene for the over-expression of carbonic anhydrase (CA12). CA12 enzymes are known to facilitate the solubilisation of extracellular aqueous carbon dioxide.[13] Since the membrane proteins are in close proximity to the SLC4A3 bicarbonate-selective transporters working with the gradient, the residual extracellular protons should induce a lowering of the local pH. The fibroblasts were also transfected to express green fluorescent proteins (GFP) as fluorescent markers to help with the identification of the cells on the microscope.

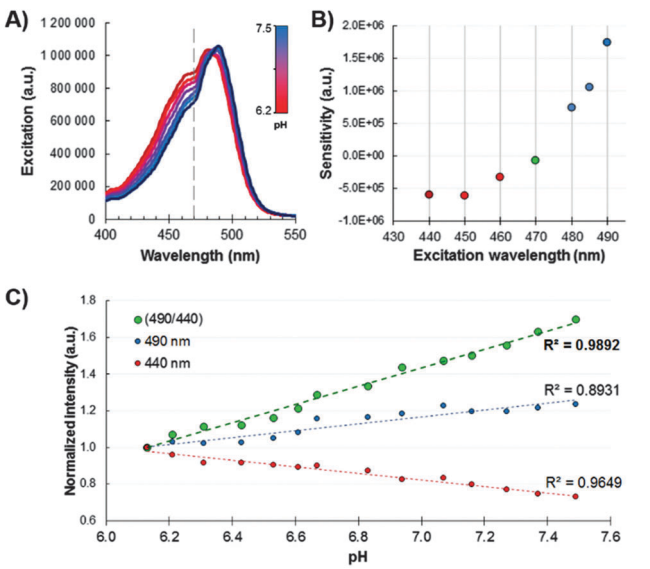

Fig. 4 (A) Excitation spectra of Ag@SiO_2-FiTC nanoprobes recorded at various pH values; the fluorescence signal was collected on the low-energy wing of the emission band of FiTC at 576 nm. (B) Sensitivity to pH measured at different excitation wavelengths; the fluorescence signal was collected at the maximum emission wavelength (512 nm). (C) Emission intensity with excitation at 490 nm (blue) and 440 nm (red), and calculated ratiometric values (green) (λ_{em} = 512 nm).

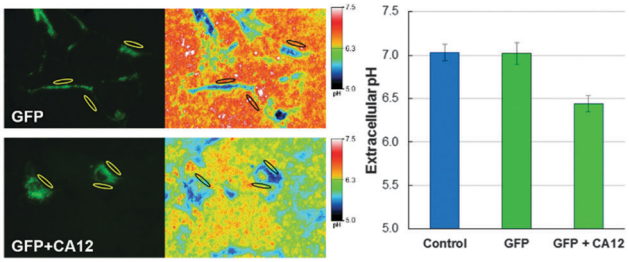

Fig. 5 Left: fluorescence images (λ_{exc} = 489 ± 6 nm, λ_{em} = 536 ± 20 nm) and ratiometric pH images (λ_{exc}: 489 ± 6 nm/436 ± 5 nm, λ_{em}: 536 ± 20 nm) of transfected fibroblasts grown on a pH-sensitive substrate. Right: ratiometric fluorescence values were measured in the regions identified by the yellow circles and converted to pH values. The error bars show standard error (N = 15). Control: unaltered cardiac fibroblasts. GFP: cells transfected with over-expressed intracellular GFP; GFP + CA12: cells transfected with over-expressed GFP and CA12 enzymes.

Unaltered, GFP- and GFP + CA12-transfected fibroblasts grown on pH-sensitive substrates in non-buffered cell culture media were imaged at an emission wavelength of 536 ± 20 nm using two different excitation filters (489 ± 6 nm and 436 ± 5 nm). Images from five regions of each sample were recorded and three ~100 μm^2 regions of interest were selected in each image, 5–10 μm away from cell membranes. Ratiometric values were converted to extracellular pH values and are shown in Fig. 5. As predicted, the increase in cell membrane activity caused by the over-expression of CA12 enzymes led to noticeable acidification of the extracellular medium, *i.e.*, from 7.0 ± 0.1 to 6.4 ± 0.1. This decrease in extracellular pH by CA12-transfected cells was confirmed by a separate flow cytometry experiment (see the ESI† for details). Similar pH values and uncertainties were measured in the extracellular space for unaltered and GFP-only cells.

Fig. 6 shows spatially-resolved pH traces measured along a 5 μm wide track leading away from the cell membrane for unaltered and GFP + CA12 transfected cells. The lower pH values recorded inside the unaltered cell are probably due to the background signal from cytosolic GFP autofluorescence which partially overlaps with the emission of FiTC. This artefact can be avoided by using a cell membrane marker with a different emission wavelength range (*e.g.*, mCherry). Interestingly, pH values measured in the extracellular space are free from interference from GFP and show a characteristic increase in pH with increasing distance from the cell,

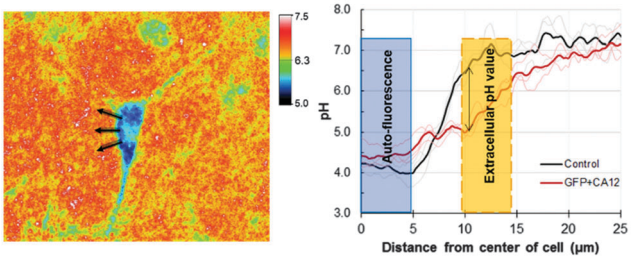

Fig. 6 Left: ratiometric pH image (λ_{exc}: 489 ± 6 nm/436 ± 5 nm, λ_{em}: 536 ± 20 nm) of a GFP + CA12 transfected cell on a pH-sensitive substrate. Right: pH values measured along 5 μm wide tracks leading away from the cell membrane (shown by the arrows) are compared for unaltered (control) and GFP + CA12 transfected fibroblast cells. Thick lines show averaged pH values. The blue and yellow boxes designate regions inside and outside the cell, respectively.

mirroring the diffusion of protons away from the membrane-bound CA12 enzymes, with a maximum difference between transfected and unaltered cells 5–10 μm away from the membrane.

Transposition of "click" chemistry was successfully optimized to functionalize silica substrates with pH-sensitive fluorescent Ag@SiO_2 probes, thus producing uniform and highly luminescent transparent devices. Measuring extracellular ion concentrations using these planar sensors offers many advantages when compared to traditional alternatives. The fluorescent Ag@SiO_2-grafted surfaces can be handled without prior training and the image processing ratiometry is easily transposable to any commercial epifluorescence microscope equipped with a camera and a basic software. The achievable spatial resolution is determined by the diffraction-limited footprint of the microscope objective and can be as small as 1 μm. Because fluorescence lifetimes are notably faster than biological mechanisms, these pH-sensitive devices can be used to study the kinetics of metabolic pathways with high temporal resolution. Moreover, plasmonic enhancement of fluorescence in core–shell nanoparticles increases luminescence intensity and resistance to photobleaching, thus allowing the prolonged analysis of cellular metabolism processes. Stable clicking of the nanoparticles on complementarily functionalized substrates nullifies the migration of ion-selective fluorophores to the cytosol and any associated cytotoxicity issues,[14] and is relevant to the study of a variety of adhesive eukaryote cells or bacterial organisms. Finally, the versatility of the fabrication procedure could lead to even more precise and more sensitive planar sensors using, for example, pH-sensitive fluorophores emitting at longer wavelengths – where auto-fluorescence interference in transfected cells is minimal – or fluorophores sensitive to other physiological ions of interest (Mg^+, Na^+, K^+, Ca^{2+}, Cl^-).

This work was supported by the Natural Sciences and Engineering Research Council of Canada, the "Fonds de la Recherche du Québec – Nature et Technologies" and the Canadian Foundation for Innovation. The authors would also like to thank M. Stephan Gagnon for help with the SEM images, and Prof. Y. De Koninck for inspiring discussions about cellular imaging.

Notes and references

1 B. A. Webb, M. Chimenti, M. P. Jacobson and D. L. Barber, *Nat. Rev. Cancer*, 2011, **11**, 671.
2 C. Geinberger and A. Konnerth, *Neuron*, 2012, **73**, 862.
3 (*a*) M. E. O'Leary and J. C. Hancox, *Br. J. Clin. Pharmacol.*, 2010, **69**, 427; (*b*) D. I. Harjes, M. Dubach, A. Rosenzweig, S. Das and H. A. Clark, *Macromol. Rapid Commun.*, 2010, **31**, 217–221.
4 C. E. Bradburne, J. B. Delehanty, K. B. Gemmill, B. C. Mei, H. Mattoussi, K. Susumu, J. B. Blanco-Canosa, P. E. Dawson and I. L. Medintz, *Bioconjugate Chem.*, 2013, **24**, 1570.
5 (*a*) C. D. Geddes and J. R. Lakowicz, *J. Fluoresc.*, 2002, **12**, 121; (*b*) K. Aslan, I. Gryczynski, J. Malicka, E. Maveeva, J. R. Lakowicz and C. D. Geddes, *Curr. Opin. Chem. Biol.*, 2005, **16**, 55; (*c*) M. L. Viger, L. S. Live, O. D. Therrien and D. Boudreau, *Plasmonics*, 2008, **3**, 33; (*d*) J. Yang, F. Zhang, Y. Chen, S. Qian, P. Hu, W. Li, Y. Deng, Y. Fang, L. Han, M. Luqman and D. Zhao, *Chem. Commun.*, 2011, **47**, 11681; (*e*) L. Rainville, M.-C. Dorais and D. Boudreau, *RSC Adv.*, 2013, **3**, 13953; (*f*) F. Magnan, J. Gagnon, F.-G. Fontaine and D. Boudreau, *Chem. Commun.*, 2013, **49**, 9299; (*g*) D. Brouard, O. Ratelle, A. G. Bracamonte, M. St-Louis and D. Boudreau, *Anal. Methods*, 2013, **5**, 6896; (*h*) Z. Bai, R. Chen, P. Si, Y. Huang, H. Sun and D.-H. Kim, *ACS Appl. Mater. Interfaces*, 2013, **5**, 5856.
6 P.-C. Lin, S.-H. Ueng, S.-C. Yu, M.-D. Jan, A. K. Adak, C.-C. Yu and C.-C. Lin, *Org. Lett.*, 2007, **9**, 2131.
7 (*a*) L. Huang, S. Dolai, K. Raja and M. Kruk, *Langmuir*, 2010, **26**, 2688; (*b*) P.-C. Lin, S.-H. Ueng, M.-C. Tseng, J.-L. Ko, K.-T. Huang, S.-C. Yu, A. K. Adak, Y.-L. Chen and C.-C. Lin, *Angew. Chem., Int. Ed.*, 2006, **45**, 4286; (*c*) D. I. Fried, A. Schlossbauer and T. Bein, *Microporous Mesoporous Mater.*, 2012, **147**, 5; (*d*) S. Prakash, T. M. Long, J. C. Selby, J. S. Moore and M. A. Shannon, *Anal. Chem.*, 2007, **79**, 1661; (*e*) N. K. Devaraj and J. P. Collman, *QSAR Comb. Sci.*, 2007, **11–12**, 1253.
8 (*a*) V. V. Rostovtsev, L. G. Green, V. V. Fokin and K. B. Sharpless, *Angew. Chem.*, 2002, **114**, 2708; (*b*) V. O. Rodionov, V. V. Fokin and M. G. Finn, *Angew. Chem.*, 2005, **117**, 2250.
9 Y. Tian, E. Fuller, S. Klug, F. Lee, F. Su, L. Zhang, S.-H. Chao and D. R. Meldrum, *Sens. Actuators, B*, 2013, **188**, 1.
10 E. D. Wieder, H. Hang and M. H. Fox, *Cytometry*, 1993, **14**, 916.
11 J. Malicka, I. Gryczynski, J. Kusba, Y. Shen and J. R. Lakowicz, *Biochem. Biophys. Res. Commun.*, 2002, **294**, 886.
12 (*a*) D. Tiedemann, U. Taylor, C. Rehbock, J. Jakobi, S. Klein, W. A. Kues, S. Barcikowski and D. Rath, *Analyst*, 2014, **139**, 931; (*b*) C. Leclerc and K. L. Wilkinson, *Environ. Sci. Technol.*, 2014, **48**, 358.
13 C. P. S. Potter and A. L. Harris, *Br. J. Cancer*, 2003, **89**, 2.
14 J. Guo, S. Xiong, X. Wu, J. Shen and P. K. Chu, *Biomaterials*, 2013, **34**, 9183.